Urban tree canopies drive human heat stress mitigation

Abstract

Climate warming and urbanisation compound the public health risk posed by heat. Heat can be mitigated at local scales through urban greening, which provides shade and reduces surface and air temperatures. Yet, the relative effectiveness of different greening options on human thermal comfort based on physiology-based indices is understudied. We installed microclimate stations at 17 locations covering a gradient of tree canopy cover and perviousness in the city of Ghent, Belgium, and monitored the modified Physiologically Equivalent Temperature (mPET) during 195 days over Spring and Summer. We assessed the canopy cover, pervious surface fraction and building sky fraction based on field measures and hemispherical pictures. Unpaved locations with trees experienced a 2.4-fold reduction in the number of days with strong heat stress (mPET > 35°C) compared to paved, treeless locations. Based on mixed models and our selected environmental variables, cooling effects were predominantly driven by tree canopy cover, where locations with 100% canopy cover had temperature maxima 5.5°C mPET lower than treeless locations throughout the monitoring period. When air temperatures rose to 40°C, cooling by tree canopies increased to 8.8°C mPET. The pervious surface fraction and building view factor were less influential, generating variation of at most 1.7°C and 1.1°C mPET, respectively. In contrast, night-time temperatures were rather determined by the regional-scale urban heat island effect than by aforementioned local factors. Still, tree canopies slightly cooled the warmest nights only, whereas the vicinity of buildings led up to 1.2°C mPET warming on average. Expanding the urban tree cover may therefore be the best solution for improving local thermal comfort levels when daytime heat peaks, but will provide little relief at night.

Keywords: Dr.FOREST; Forest Microclimate; Heat Stress; Nature-Based Solution; Thermal Comfort; Urban Microclimate.

Introduction

People are increasingly exposed to extreme heat levels as climate warming progresses. Under current policies, around 4 ± 2% of the global population will face ‘unprecedented heat’ (over 75 days with maxima above 40°C per year) by 2030, increasing sharply to 23 ± 9% by 2090 (Lenton et al., 2023). Such heat strains the cardiovascular, renal and respiratory system, with potentially fatal outcomes for, particularly, infants, the elderly and people with a range of pre-existing physical or mental conditions (Ebi et al., 2021). From 2000 to 2017, heat-related mortality in the elderly already increased by 68% globally (Romanello et al., 2022), which will worsen as about half of the global population will be exposed to heat surpassing lethal thresholds even under most stringent mitigation scenarios by 2100 (Mora et al., 2017).

Heat risks are heterogeneously distributed. At the global scale, people most vulnerable to heat also tend to be those least responsible for global warming (Lenton et al., 2023). At the regional scale, the Urban Heat Island effect (UHI) turns cities into heat hotspots. The UHI is generated because: i) human-made heat is added to the environment (e.g. from motorised traffic and air-conditioning), ii) incoming solar radiation is more effectively absorbed by urban infrastructure with low albedo and high thermal admittance, iii) heat is less easily released back, iv) air pollution absorbs and gives off additional long-wave radiation, v) the lack of pervious surfaces and vegetation reduces the share of energy converted to latent heat and, vi) reduced wind speeds hamper turbulent heat exchanges (Kleerekoper et al., 2012; Oke, 1973; Stewart and Oke, 2012). The UHI is particularly pronounced at night, when trapped solar radiation is slowly emitted as longwave radiation (Deilami et al., 2018). Nightly heat presents a health hazard by itself because it interferes with sleep quality and therefore the body’s recovery capacity (Obradovich et al., 2017). Ongoing urbanisation compounds the threat of global warming, because expanding the urban fabric will exacerbate UHI effects (Wang et al., 2019) and because the global rural-to-urban migration (United Nations, 2019) will expose a quickly growing number of people to UHI-amplified heat.

Technological solutions such as human-made shading structures, reflective surfaces and misting devices can mitigate heat at the local scale (Taleghani, 2018; Turner et al., 2023; Vanos et al., 2022). They do this by, respectively, shading passers-by, reducing stored solar radiation and reducing the air temperature via latent heat transfer (Taleghani, 2018; Wong et al., 2021). However, these costly interventions are resource-intensive in terms of energy, materials and water, and the same can be achieved via more cost-effective nature-based solutions such as grasslands, green walls and roofs, isolated single trees and groups of trees. Each of these has the potential to reduce the share of solar energy intercepted and stored by human-made surfaces, and to lower air temperatures via evapotranspirative cooling, while single trees and groups of trees additionally provide shade (Taleghani, 2018; Wong et al., 2021). The cooling effect of trees has real impact, exemplified by a recent Europe-wide study that found 40% of UHI-related deaths to be preventable should cities guarantee a 30% canopy cover (Iungman et al., 2023).

Since urban greening has great potential to safeguard humans from heat, there is interest in comparing cooling capacities of existing greenspace types. A large remote sensing study found that tree canopy surface temperatures were 8-12°C cooler than grey surfaces during hot extremes in European cities, which was two to four times cooler than treeless greenspaces (Schwaab et al., 2021). Yet, surface temperatures poorly predict how a human body will physically perceive temperature, since the latter is defined by air temperature, mean radiant temperature (representing short- and longwave radiation reaching the body), air humidity and wind speed (Johansson et al., 2014; Mayer and Höppe, 1987). The integrated effect of these variables is typically proxied using so-called physiological thermal indices, with most notable examples being the Universal Thermal Climate Index (UTCI) and the Physiologically Equivalent Temperature (PET) (Potchter et al., 2018).

Ground-based monitoring studies applying such indices exist, but they are often limited in their spatio-temporal coverage and thus also statistical power. For example, cooling effects by vegetation were reported based on four contrasting locations in the Singapore Botanical Gardens (Chow et al., 2016) and on six well-spread locations in Ghent, Belgium (Top et al., 2020). One of the largest studies was done in four cities in the Czech Republic, where at most three hot days were monitored on 17 locations (Lehnert et al., 2020). Furthermore, these studies provide only qualitative descriptions of green elements (e.g. 'urban park' or 'valley lined with palms'). Together, this restricts the capacity to attribute cooling capacities to specific environmental factors, both anthropogenic or natural, and in a quantitative manner.

Here, we monitored 195 days of local thermal conditions at 17 different locations within a single neighbourhood (in Ghent, Belgium) that range from completely 'grey' (i.e. a paved industrial site) to completely 'green' (i.e. a small woodland). Location characteristics were described quantitatively using methods from urban planning and forest ecology. The main aim was to quantify the relative cooling potential of different types of grey- and greenspaces at the local scale, thereby identifying the most effective cooling solutions.

Materials & Methods

Study design and locations

Study locations were situated in Ekkergem (51°03'06"N, 3°42'22"E), a mostly residential neighbourhood of Ghent, Belgium, that also houses a university campus. Based on measures between 1991 and 2020, Ghent has a mean annual temperature of 10.9°C and the hottest month is July, whose minimum, mean and maximum temperatures reach, respectively, 13.4°C, 18.4°C and 23.4°C (Royal Meteorological Institute of Belgium, 2023). In the year we conducted the study, the summer was particularly hot in Belgium. Since monitoring by the RMI began in 1892, the summer of 2022 was within the top three summers concerning the number of 'Summer days' (36 days above 25°C), 'tropical days' (12 days above 30°C), the mean Summer temperature (19.6°C) and the mean Summer maxima (24.7°C) (KMI, 2022, p. 202).

Seventeen locations were selected (Fig. 1). To maximise the contrast in locations and to disentangle the effects of trees from the effects of shading by buildings and cooling by non-tree greenery, four categories were made: i) mostly paved and minimally vegetated (n = 6, hereafter 'paved & grey'), ii) mostly paved with trees (n = 3, 'paved & trees'), iii) mostly unpaved with low vegetation like lawns or a minimal influence of small trees (n = 3, 'unpaved & low green'), and iv) mostly unpaved with multiple trees (n = 5, 'unpaved & trees') (Fig. 1). Since variation was still present within these categories, a gradient was obtained from treeless to treed, and from intensely paved to unpaved (Table 1). The 'greenest' location was a small but fully-developed private forest (Fig. 1C), while one of the 'greyest' locations was a large parking area between university buildings (Fig. 1D). Attention was also paid to have a similar number of N-S or E-W oriented streets. Local Climate Zone (LCZ) classifications (Stewart and Oke, 2012) were added to Table 1.

Two types of controls were used to compare local-level urban heat stress measures. First, data were obtained from the nearest synoptic weather station of the Royal Meteorological Institute of Belgium (RMI), which is located in Melle (RMI code 6434), a rural location c. 11km from Ekkergem. These are air temperature measures conducted at 2m height above a short lawn. They thereby serve as a comparison between our local temperature measures and typical temperature conditions as reported to the broader public e.g. via weather forecasts. The second control measures come from microclimate stations identical to the loggers installed in Ekkergem, but located in ten forest stands of the TREEWEB network (De Groote et al., 2017), which were also studied by Gillerot et al. (2022). The forests are scattered roughly 10-20 km south of Ekkergem in a rural landscape, and can be considered representative for managed mature forest stands of the region. They are dominated by the tree species *Fagus sylvatica*, *Quercus robur* and *Q. rubra*, either as monospecific stands or mixtures. Their microclimatic data were averaged into a single time series, representing an "average, mature rural forest".

Human heat stress measures

The meteorological factors required for an accurate assessment of human thermal comfort are air temperature and humidity, wind speed and mean radiant temperature (T_{mrt}) (Johansson et al., 2014; Mayer and Höppe, 1987). These variables were measured at the local level using one self-made microclimate station per location (n = 17). Sensors were mounted on wooden poles at 1.1m height, representing the average centre of gravity of an adult human body (ISO, 1998; Johansson et al., 2014). Air temperature and humidity were monitored using Lascar EasyLog EL-USB-2 sensors (accuracy ± 0.45°C and ± 2.25%, respectively), mounted in tubular PVC radiation shields and oriented towards the north (Zellweger et al., 2019). Wind speed was monitored using a cup anemometer coupled to a Lascar Easylog EL-USB-5 logger. T_{mrt} requires the grey globe temperature (Thorsson et al., 2007). It was obtained by using a thermocouple type T connected to a Lascar EasyLog EL-USB-TC (accuracy ± 1.0°C), which was inserted into a 40 mm diameter acrylic ball coated in RAL 7001 paint (Thorsson et al., 2007). This roughly represents how a clothed human body would intercept short- and longwave radiation from the environment, and its small diameter makes it more responsive to the quickly changing outdoor environment than the standard 150 mm black globes (Aparicio et al., 2016; Nikolopoulou et al., 1999). With this grey globe temperature, T_{mrt} can be calculated based on a formula adapted for the outdoors (Thorsson et al., 2007):

$$T_{mrt} = \left[(T_g + 273.15)^4 + \frac{1.335 * 10^8 {V_a}^{0.71}}{\varepsilon * D^{0.4}} * (T_g - T_a)\right]^{\frac{1}{4}} - 273.15$$

where T_g is the globe temperature (°C), V_a is the wind speed (m/s), ε is the globe emissivity (0.97), D is the globe diameter (0.04 m) and T_a is the air temperature (°C).

Meteorological factors were measured every 15 minutes at each location. However, due to logistic constraints, wind speed was only measured in one plot (HG4; see Table 1). This is a caveat, since wind can vary significantly across sites. Recordings span from March 19th until September 30th 2022 (195 days), to ensure that hot periods would be covered and could be compared to moderate conditions in Spring and generally throughout the monitoring period. An exception is plot IV5, which was installed on May 20th. To buffer out some short-term fluctuations and to obtain smoother temperature trends, a centre-aligned rolling average was applied with a window of five observations (i.e. the average of a given timestamp and the four half hours around it). For further methodological details, the sensor calibration procedure and discussions on data quality, please refer to Gillerot et al. (2022).

Perceived temperature was quantified using the modified Physiological Equivalent Temperature (mPET) (Chen and Matzarakis, 2018). Similar to PET, the most commonly used thermal index in research (Potchter et al., 2018), it is based on the human body's energy balance and it considers the effects of the aforementioned meteorological conditions (Höppe, 1999; Mayer and Höppe, 1987). It benefits from being applicable to conditions ranging from extremely cold to extremely hot, and it is expressed in degrees Celsius, which makes it easily interpretable (Matzarakis et al., 1999). It can then be used to derive heat stress levels based on thermal stress categories (Matzarakis et al., 1999). One of the main differences with PET is that mPET will adapt the clothing factor of the model body in function of thermal conditions (Chen and Matzarakis, 2018). As conditions become hotter, the model will assume that the average person will reduce their clothing insulation adaptively, which ultimately generates more realistic and more buffered (conservative) thermal stress values. Potentially, more advanced and accurate thermal indices are available (Potchter et al., 2018), but we assume that the usage of mPET will provide a robust reflection of relative differences between locations – which is the focus of this study. mPET values were calculated in RayMan V3.1 (Matzarakis et al., 2010, 2007).

Site characterisation

Site characteristics were quantified within circular plots with 10m diameter, using the microclimate station as the centre. A set of complementary measures aimed to describe the grey and green elements within the plot. Tree and forest measures were focused on their vegetation structure, with particular attention for the canopy cover given that this was the dominant driver for heat stress mitigation in European forests (Gillerot et al., 2022). In this paper, canopy cover relates to trees larger than 2m exclusively, distinguishing it as a shade-casting vegetation type (e.g. hanging plants were not considered).

First, the surface characteristics were described by visually assessing the share of each surface type (e.g. asphalt, grass, water). These were then categorized according to perviousness (i.e. being penetrable by water) to obtain the 'pervious surface fraction' (%). Second, we visually estimated the height (m) and measured the distance (m) of each structure (e.g. building, tree) in each cardinal direction relative to the sensors. These were not included in further analyses but allowed to interpret unexpected findings. Next, using forest ecology methodologies, we measured the circumference of trees in the plot to calculate the local basal area, which is a common measure representing the cross-sectional area of tree stems at breast height per hectare. Species-specific canopy cover was estimated based on the vertical projection of crowns (Zellweger et al., 2019). At last, five hemispherical pictures were taken with a Nikon D90 camera and a 180° hemispherical lens: one at the centre of the plot and then one in each cardinal direction at 5m from the centre. Rather than calculating the sky view factor, a common variable in biometeorology, the 'building view factor' (%) was obtained instead (see e.g. (Yan et al., 2022) with pictures processed in Gap Light Analyzer 2.0 (Frazer et al., 1999). This was to disentangle shading effects by trees and buildings. An overview of the locations and their most important environmental characteristics is given in Table 1.

Data analysis

Mean thermal conditions (air temperature and mPET) were calculated for two distinct periods within the day: night (12pm – 6am) and afternoon (12am – 6pm). Similarly, data were summarised to day-level values (max, min, mean and 95th percentiles of warmest and coldest readings for a less strongly fluctuating values). These daily data were used to count the number of days for which maxima fell into thermal stress categories defined by Matzarakis et al., (1999) per location type. Also based on daily values, offset values were calculated (urban minus rural control conditions), which is a standard procedure in microclimate ecology to facilitate statistical analyses and to render buffering effects more explicit and interpretable (De Frenne et al., 2021). The rural forest measures (mPET) served as control conditions to compare urban conditions to 'maximally green' rural conditions. Offsets were also calculated using RMI weather station data, but focused on air temperature.

Canopy cover, pervious surface fraction and building view factor were selected as the main complementary predictor variables based on exploratory analyses. Our assumptions regarding the causal dependencies between variables are presented in the Directed Acyclic Graph (Fig. 2). We tested whether this DAG was consistent with the data by assessing the conditional independence statements implied by the DAG and found that our data were consistent with it (Text S1). We then applied the backdoor criterion (Arif and MacNeil, 2023) which showed that a multiple regression model with all three environmental predictors (see next paragraph) was sufficient to estimate the causal effect of each predictor on temperature. Alternative DAGs were tested including, for example, a version where the building view factor is not causally related to the canopy cover, but these failed the tests of conditional independence (Text S1). Moreover, debate around the directionality of causal relationships between the predictors is possible (e.g. the presence of buildings could be considered to determine the potential canopy cover, but the opposite reasoning is also possible), but we assume that this has no consequences for their direct effects on thermal conditions in this case.

Using offset values as response variables (max, min or means of night or afternoon periods), the effects of environmental predictors were modelled using Linear Mixed Models (LMMs), selected following Zuur et al. (2009). Predictors were both tested alone and removed from the full model, to verify the robustness of effects and their predictive power. Control temperatures were also added as a predictor and were allowed to interact with other predictors in additional models because offsets tend to vary strongly with macroclimatic conditions (De Frenne et al., 2021). LMMs included 'location' as a random factor, and a correlation structure of the form corAR1(form = ~ 1 | plot) to account for the daily repeated measures.

Significance levels were tested via restricted maximum likelihood estimation (Zuur et al., 2009). To render effect sizes of the three main predictor variables more explicit, predictions over the observed range of the target variable were made while keeping the two non-target variables at their mean value. The LMMs were built using the packages *nlme* (Pinheiro et al., 2021) and *lme4* (Bates et al., 2015), using the programme R version 4.3.0 (R Core Team, 2023).

Results

Effect of canopy cover during heatwave conditions

The summer of 2022 was exceptionally hot, with July 19th being the hottest day of the year (Fig. 3A), yielding air temperatures up to 38.4°C at the nearest RMI weather station. At the local scale, most of our measurements were multiple degrees Celsius warmer in air temperature than official reporting (data not shown). A second period of interest was the second heatwave of the year (9th until 16th of August), for which the hottest days were selected (Fig. 3B). Especially during this second heatwave, a large UHI was captured at night. The night from the 10th to the 11th, the average urban location was about 4°C warmer in air temperature than official readings outside the city, and the two subsequent nights were about 7°C warmer.

Trends in perceived temperatures revealed very large contrasts between locations. On the 19th of July (Fig. 3A), the hottest location (HG5) reached 41.5°C mPET, which is 7.0°C mPET warmer than the maximum value reached on the coolest location (HG2). During the second heatwave (Fig. 3B), these differences were even further exacerbated, with differences of around 12°C mPET for all three days. The canopy cover seems to explain a substantial share of this variation (see statistical results below), where especially the highly covered (> 50%) locations are multiple degrees cooler. The rural forest controls approximately follow the temperature trend of the coolest urban location, albeit with moderately lower values at night. Nightly mPET values seem generally less contrasting and little associated with canopy cover based on day-to-day mPET curves.

Comparison with rural forest conditions

The overall mean mPET temperature was warmer than rural forest controls for 16 out of our 17 urban location on warm days, where maxima also increasingly diverged with increasing temperatures. Under moderate heat stress in rural forests, the average 'paved & grey' location was 5.9°C mPET warmer (Fig 4A). 'Paved & trees, 'unpaved & low green' and 'unpaved & trees', were warmer by, respectively, 3.2°C, 6.3°C and 2.0 °C. The presence of trees appears to be a dominant factor (Fig. 4B).

Night-time urban mPET readings were between 0.5°C and 1.6°C warmer than rural forests, with less variation among location types. Nonetheless, perviousness seems more influential than the presence of trees when it comes to nightly conditions.

Number of days with heat stress

On average, the most urbanised locations ('paved & grey') experienced 141 days (out of 195) with slight heat stress or more (PET > 23°C), and 11.5 days with strong heat stress or more (PET > 35°C) (Fig. 5). The greenest locations ('unpaved & trees') experienced much less heat stress with, respectively, 101 days with slight and 4.8 days with strong thermal stress. Unexpectedly, locations in the 'unpaved & low green' category resemble 'paved & grey' locations and even have slightly more heat days, while 'paved & trees' and 'unpaved & trees' locations are more alike based on the mean number of days. Again, tree presence emerges as a dominant driver.

Average night-time temperatures show a different picture, where 'paved & grey' locations had the most numerous warm nights (61 nights with mPET above 18°C), followed by 'paved & trees' (59 nights), 'unpaved & trees' (50 nights) and 'unpaved & low green' (49 nights). This suggests again that the perviousness may be the most influential factor during nights.

Effects of canopy cover, pervious surface fraction and building view factor

Concerning daily maxima, canopy cover emerged as the strongest predictor variable ($\beta = -0.055$, $t = -13.657$, $p < 0.0001$), followed by pervious surface fraction ($\beta = 0.017$, $t = 4.576$, $p = 0.0005$) and building view factor ($\beta = 0.016$, $t = 2.169$, $p = 0.0493$). The model explained a large share of variation ($R^2_{marginal} \approx R^2_{conditional} = 0.83$). Repeating analyses for the 95th percentile of warmest readings per day led to very analogous but slightly lower model coefficients (Text S2). When testing interactions between environmental characteristic variables and RMI control measures, canopy cover was the only predictor to significantly vary with control conditions ($p < 0.001$). This suggests that canopy cover's effect increases as official weather station readings rise.

Compared to an average location (building view factor = 23.3% and pervious surface fraction = 46.8%) without any canopy cover, a 100% canopy cover leads to an average temperature maxima *decrease* of 5.5°C mPET. Doing the same for the pervious surface fraction and building view factor (mean canopy cover = 26.3%), an *increase* in mPET of, respectively, 1.7°C mPET and 1.1°C mPET is expected for a fully pervious ground surface and for a building-surrounded location. Doing the same but including the interaction between canopy cover and official weather station readings, a 100% canopy cover under air temperatures of 20°C, 30°C and 40°C, leads to respective cooling magnitudes of 5.3°C, 7.1°C and 8.8°C mPET.

Concerning afternoon averages (12pm - 6pm), only canopy cover had a significant cooling effect ($\beta = -0.038$, $t = -2.487$, $p = 0.027$). This corresponds to a reduction of 3.8°C mPET in afternoon averages for a fully covered location compared to an average treeless location.

Concerning nightly minima, environmental predictors had much less explanatory power ($R^2_{marginal} \approx R^2_{conditional} = 0.21$). The final model only had significant effects for the interaction between RMI minima and canopy cover ($p < 0.0001$) and between RMI minima and pervious surface fraction ($p < 0.0001$). Repeating analyses for the 95th percentile of coldest readings per day led to very analogous results (Text S2) When the RMI station reports a daily minimum of 10°C, a fully canopy-covered location is predicted to be 0.6°C mPET warmer than a treeless location. At 20°C, this becomes a slight cooling effect of 0.05°C mPET, with tree canopies leading to stronger cooling as these minima increase and vice-versa. The opposite is observed for the pervious surface fraction: a fully pervious location will be 0.4°C mPET cooler under a daily minimum of 10°C and 0.1°C mPET warmer under 20°C compared to a fully impervious location.

Concerning nightly averages (12am – 6am), only the building view factor had a significant effect ($p = 0.023$). Compared to a location devoid of buildings, the location with the highest building density based on our data (i.e. 69.1%) is predicted to be 1.2°C mPET warmer. No significant interactions with control temperatures were found.

Discussion

Based on 195 days of *in situ* monitoring of contrasting urban microclimates, we found that tree canopy cover dominated human heat stress mitigation compared to the building view factor and pervious surface fraction. Compared to our average treeless location, a full canopy cover reduced daytime heat maxima by a mean 5.5°C mPET throughout the monitoring period, rising to 8.8°C mPET when air temperatures reached 40°C. The building view factor and pervious surface fraction led to moderate warming effects. Nightly mPET values were comparatively little influenced by aforementioned local-scale variables.

Effects of canopy cover

Evidence from this study and existing literature suggests that canopy cover much more effectively reduces local heat stress than the imperviousness and shading by buildings. A modelling study for Freiburg, Germany, found trees to reduce PET by 3.0°C on average (max. 17.4 °C) while grasslands only achieved a 1.0°C (max. 4.9°C) reduction (Lee et al., 2016). A remote sensing study of European cities found the cooling capacity of trees to be up to four times more potent than treeless greenspaces based on surface temperatures (Schwaab et al., 2021). Using an observational setup and a thermal index similar to ours (UTCI), a multi-city Czech study reported a mean cooling of 5.5-8.5°C UTCI below trees, whereas lawns were only about 0.9°C cooler - both compared to unshaded impervious locations (Lehnert et al., 2020). Another study found UTCI to be reduced by 4.7°C under broadleaf- and 4.5°C under coniferous trees, whereas green roofs and walls could at most reach a cooling of 0.2°C (Geletič et al., 2022). Although we used mPET, both absolute cooling magnitudes and relative differences between greenspace types are very similar to our findings.

Even small single trees made a noticeable difference, but strongest cooling seems especially achieved under high canopy covers (i.e. share of sky area covered by tree canopy biomass) (Fig. 3). Using a modelling approach, a review found that air temperatures drop by around 0.3°C for each 10% increase in canopy cover (Krayenhoff et al., 2021). An observational study in Madison, US, found fully covered locations to be 0.7-1.5°C cooler in air temperature than treeless locations (Ziter et al., 2019). They also found that the effect of canopy cover was non-linear, with canopy cover being disproportionately more effective beyond a 40% cover. This is also suggested by our data, where especially the locations with canopy cover > 50% strongly diverge from treeless conditions (Fig. 3). Corroborating these findings, a Chinese study found that streets with 13% canopy cover experienced strong heat stress (> 35°C PET) for about two-thirds of the time on hot summer days, while such heat stress was never reached in streets with 75% canopy cover, which were on average 13.7°C PET cooler (Ren et al., 2021). We too observed that the presence of trees prevented the occurrence of extreme heat stress (PET > 41°C). Monitoring of the microclimate in 131 rural forest stands also found canopy cover to most strongly cool PET levels, further reinforcing its dominant role in thermal buffering (Gillerot et al., 2022). Besides canopy cover, indices for canopy density have also been found to be influential (Rahman et al., 2020), though a recent study found that their effect may be outweighed by canopy cover (Tamaskani Esfehankalateh et al., 2021).

Effect of Pervious Surface Fraction and Building View Factor

Although only modestly influential based on our data, existing literature suggest that both pervious surface fraction and Building View Factor also have significant heat mitigation potential. Comparable studies using physiological indices like mPET, however, remain rare (e.g. He et al., 2015; Yan et al., 2022).

Warmer conditions are often found with increasing imperviousness, partly contrasting our results. Already in 1972, a study measured a surface temperature difference of 15.5°C between a weed field and a parking lot on a clear summer day at noon (Landsberg and Maisel, 1972). Interestingly, the air temperature did not differ at noon, while it was slightly warmer in the parking lot at midnight (Landsberg and Maisel, 1972) because such impervious surfaces effectively emit trapped heat at night (Taleghani, 2018). More recently, fully impervious locations were found to be up to 1.3°C warmer in air temperature compared to fully pervious locations in a mid-sized U.S. city (Ziter et al., 2019). Similarly, increasing the pervious surface fraction by 10% was found to increase the median UHI maxima by 0.22°C in Rotterdam during summer months (van Hove et al., 2015). Our results confirm that perviousness has a cooling effect by night (air temperature < 20°C), but suggest an unexpected warming effect by day. This could partly be due to our definition of perviousness, which does not exclude unvegetated, compacted and low albedo surfaces (e.g. trampled bare soil as in plot LG3). Alternatively, it could be related to low soil water content during summer 2022, the driest on record (KMI, 2022), since the cooling capacity of pervious surfaces is driven by soil water availability (Resler et al., 2021). Warming could also be generated by confounding indirect effects such as window-reflected sunlight on the lawn of plot LG2 (see 'strengths, limitations & recommendations') (Taleghani, 2018). Such location-specific effects emphasise the need for comprehensive spatial replication.

Most studies use the Sky View Factor (SVF) instead of the building view factor, which can include vegetation effects and should therefore be compared with caution. A suitable comparison with minimal vegetation effects is a study in Hong Kong which found a negative relationship between the SVF and the air temperature, where a 15% increase in SVF would lead to a decrease of 1°C (Chen et al., 2012). Another study (this time with a confounding tree effect) found the SVF to explain daytime differences of up to 4°C PET over a SVF range from ~0.26 to 0.6, but the relationship was non-linear and inconsistent (He et al., 2015). Based on vast spatial coverage, (Yan et al., 2022) found that an increased SVF led to i) warming by day because of lower shading potential and ii) cooling by night because an open sky facilitates the dissipation of stored longwave radiation (Chen et al., 2012). However, the SVF can be separated into a building and tree component, as we have done as well, leading to very diverging results. Indeed, the building sky fraction was found to warm both day- and night-time air temperatures, while the 'tree view factor' cooled daytime temperatures and had little effect at night (Yan et al., 2022). This is almost exactly what we found based on mPET, except for an additional cooling effect by trees at night when air temperature minima reach 20°C or higher. While both buildings and trees can provide shade, distinguishing their effects is important because buildings are effective radiation traps whereas trees provide additional evapotranspirative cooling (Taleghani, 2018; Wong et al., 2021).

Comparison with controls and night-time cooling

Comparing rural forest controls (Fig. 3) yielded unexpected results. Rural and urban forest temperatures were comparable during daytime, although we had expected urban forests to be warmer than their rural counterparts for two reasons. First, we expected urban forests to be warmed by the UHI and second, their small surface area would lead to strong 'edge effects' (i.e. forest edges being less buffered than interiors), which were shown to reach at least 50m from the edge in European urban forests (De Pauw et al., 2023). The UHI, being stronger at night, may have had little influence on daytime temperatures (but see cases reviewed in Tzavali et al., 2015), and our studied urban forest locations may have been so thoroughly covered by canopies as to obscure strong edge effects. Another unforeseen result is that differences between the most urbanized and the most canopy covered locations rarely exceeded 10°C mPET, while we expected this to be much higher than the contrasts of 14.5°C PET found when comparing forests to a fully pervious lawn without woody vegetation (i.e. the most common control condition in forest microclimate research (De Frenne et al., 2021)) under rural circumstances (Gillerot et al., 2022). This is most likely due to the usage of mPET instead of PET. Indeed, when repeating analyses using PET, maximal differences of well over 15°C PET are found between the coolest and hottest locations. In sum, mPET strongly buffers out hot extremes, at least partly because of the automatic clothing model (Chen and Matzarakis, 2018), making it a rather conservative estimate of cooling capacities.

Based on statistical analyses, but also clearly visible on selected hot days (Fig. 3), environmental factors (i.e. canopy cover, building view factor, pervious surface fraction) have much less effect on nightly mPET. In contrast to daytime conditions, all three environmental factors had significant yet modest effects - depending on whether mPET minima or nightly means were considered. This is very much in line with results by Ziter et al. (2019) who found a lower air temperature variation by night, and a maximal night-time cooling by pervious surface fraction of 0.7°C. Another study found that a park's surface temperature was 8°C cooler during daytime, but only 2°C at night (Nichol, 2005). A review confirms that urban trees are substantially less influential at night and could sometimes even lead to slight warming depending on the specific context (Krayenhoff et al., 2021). This was recently also observed in an Australian study (Sharmin et al., 2023) and during a few night-time hours in a Czech study, though trees provided cooling when considering the whole night (Geletič et al., 2022). Yet, comparing our local air temperatures to RMI control measures shows that night-time temperatures seem mostly dictated by a strong UHI effect – which is in line with literature (Deilami et al., 2018). Top et al. (2020) found it to reach maximally 8.7°C in air temperature, also in Ghent, which is similar to our findings. This nightly UHI effect is less visible based on our rural forest controls (Fig. 3), because forests also buffer daily minima, keeping their microclimate significantly warmer than surrounding open rural spaces where official weather stations would typically be located (De Frenne et al., 2021, 2019).

Strengths, limitations and recommendations

We quantified environmental conditions at a very local scale within a single city. This allowed for making precise predictions concerning the relative roles of various environmental conditions, but this restricts the generalizability beyond our characterised perimeter. Inhabitants, and especially those vulnerable subgroups that might shelter mostly indoors, may spend only limited time at those specific locations (i.e. sidewalks, parks, squares) (Wanka et al., 2014), limiting the relevance for people's health. This may be addressed by coupling local measures to remotely-sensed landscape-scale metrics, including all three environmental variables studied here. Yet, extrapolating our data to wider areas will nonetheless probably yield analogous results. For example, an observational study found that variation in air temperature reductions could increasingly be explained by canopy cover and pervious surface fraction as the radius of buffer areas increased until 60-90m (Ziter et al., 2019).

Additionally, our final selection of three environmental variables (i.e. canopy cover, pervious surface fraction and building view factor) may have failed to capture other significant environmental effects. For example, we have not examined the influence of the more fine-grained types of impervious and pervious surfaces, nor did we measured the thermal properties of human-made infrastructure surrounding our sensors. However, we believe that our variable selection covers the most important environmental characteristics, as is also suggested by the large share of variation explained by our models (R^2 = 0.83).

Two locations presented unexpected brief temperature spikes at similar times in the day during some consecutive days. Based on the timing, the orientation and the trends in grey globe temperature, the spikes at locations LG2 and HG1 are probably caused by, respectively, reflection of the morning sun in the nearby building's windows and reflection of the afternoon sun in the pond water. The occurrence of such unexpected findings emphasises the importance of an adequate replication of locations and a thorough characterisation of the environment.

Besides the spatial limitations, the monitoring of a single year may also have reduced representativeness. Indeed, the summer of 2022 was exceptionally hot and dry (KMI, 2022), which, for example, may have impeded the cooling potential of vegetation due to reduced transpiration. Conversely, that summer provided an interesting case-study, given that it may better represent near-future conditions.

One major strength of the current study is the usage of low-cost microclimate stations (EUR <150) allowing for a larger spatial and temporal coverage (battery longevity > 2 years) than the bulk of existing observational studies using advanced weather stations. Auspiciously, the development of cheap sensors is quickly rising (Krüger et al., 2023), which is particularly interesting if these are coupled to long-term monitoring of a comprehensive range of thoroughly characterised urban microenvironments (Beele et al., 2022). This enables identifying consistent patterns using statistical approaches, whereas single observations on per location type will hardly manage to disentangle causal factors. Noteworthy, however, is that measurement accuracy of our setup may be lower than WMO standards – making our low-cost sensors also a potential weakness.

Management implications

Based on our data for a mid-sized Belgian city and based on existing local and remote sensing research, daytime heat is clearly most effectively mitigated by expanding the urban tree canopy cover. Important cooling benefits would consequently be reached in cities that comply with the '3-30-300 rule', which advocates that every resident should be able to see at least three trees from their home, that their neighbourhood has a minimum of 30% canopy cover, and that their nearest greenspace larger than 0.5 ha is maximum 300m away (Konijnendijk, 2021). In line with these recommendations, a study on the air temperature of 93 European cities found that guaranteeing a 30% canopy cover would reduce UHI-related deaths by roughly 40% (Iungman et al., 2023). Yet, but perhaps unrealistic for many cities, other scholars and us have found that especially canopy covers of 40-50% and higher have a disproportionate cooling effect (Ren et al., 2021; Ziter et al., 2019) – at least at the local scale. Given that canopy cooling effects are particularly strong at the local scale and during daytime, extra attention could be paid to guarantee the presence of trees at locations where people spend most time during peak heat moments of the day (e.g. benches and busy streets).

Preventable heat death numbers could dwindle even further at those higher canopy cover levels, but urban planning interventions may first prioritise the equitable distribution of urban trees and forests. Indeed, neighbourhoods of lower socio-economic status tend to be more exposed to heat stress while its residents have less material and social resources guaranteeing their heat resilience (Harlan et al., 2006).

Conclusions

Our investigation of urban microclimates during the summer of 2022 underscores the pivotal role of tree canopy cover in mitigating human heat stress. The study's strengths lie in its meticulous local-scale analyses, leveraging low-cost microclimate stations for expansive coverage. Fully canopy-covered locations were remarkably cooler, reducing daytime maxima with 5.5°C mPET on average and reaching 8.8°C mPET during extreme heat conditions. This contrasts with modest effects from pervious surface fraction and building view factor. Nighttime temperatures, primarily influenced by the UHI, exhibited less sensitivity to these local environmental variables. Our findings underscore the critical importance of securing a local minimal canopy cover of 30% and preferably even more to safeguard urbanites from increasingly prevalent heat hazards at the local scale.

References

Aparicio, P., Salmerón, J.M., Ruiz, Á., Sánchez, F.J., Brotas, L., 2016. The globe thermometer in comfort and environmental studies in buildings. Revista de la Construcción 15, 57–66. https://doi.org/10.4067/S0718-915X2016000300006

Arif, S., MacNeil, M.A., 2023. Applying the structural causal model framework for observational causal inference in ecology. Ecological Monographs 93, e1554. https://doi.org/10.1002/ecm.1554

Bates, D., Bolker, B., Walker, S., 2015. Fitting linear mixed-effects models using lme4. J Stat Softw 67, 1–48.

Beele, E., Reyniers, M., Aerts, R., Somers, B., 2022. Quality control and correction method for air temperature data from a citizen science weather station network in Leuven, Belgium. Earth System Science Data 14, 4681–4717. https://doi.org/10.5194/essd-14-4681-2022

Chen, L., Ng, E., An, X., Ren, C., Lee, M., Wang, U., He, Z., 2012. Sky view factor analysis of street canyons and its implications for daytime intra-urban air temperature differentials in high-rise, high-density urban areas of Hong Kong: a GIS-based simulation approach. International Journal of Climatology 32, 121–136. https://doi.org/10.1002/joc.2243

Chen, Y.-C., Matzarakis, A., 2018. Modified physiologically equivalent temperature—basics and applications for western European climate. Theor Appl Climatol 132, 1275–1289. https://doi.org/10.1007/s00704-017-2158-x

Chow, W.T.L., Akbar, S.N. 'Assyakirin B.A., Heng, S.L., Roth, M., 2016. Assessment of measured and perceived microclimates within a tropical urban forest. Urban Forestry & Urban Greening 16, 62–75. https://doi.org/10.1016/j.ufug.2016.01.010

De Frenne, P., Lenoir, J., Luoto, M., Scheffers, B.R., Zellweger, F., Aalto, J., Ashcroft, M.B., Chistiansen, D., Decocq, G., Pauw, K.D., Govaert, S., Greiser, C., Grill, E., Hampe, A., Jucker, T., Klinges, D., Koelemeijer, I., Lembrechts, J.J., Marrec, R., Meeussen, C., Ogee, J., Tyystjärvi, V., Vangansbeke, P., Hylander, K., 2021. Forest microclimates and climate change: importance, drivers and future research agenda. Glob. chang. biol.

De Frenne, P., Zellweger, F., Rodríguez-Sánchez, F., Scheffers, B.R., Hylander, K., Luoto, M., Vellend, M., Verheyen, K., Lenoir, J., 2019. Global buffering of temperatures under forest canopies. Nat Ecol Evol 3, 744–749. https://doi.org/10.1038/s41559-019-0842-1

De Groote, S., van Schrojenstein Lantman, I., Sercu, B., Dekeukeleire, D., Boonyarittichaikij, R., Smith, H.K., De Beelde, R., Ceunen, K., Vantieghem, P., Matheve, H., De Neve, L., Vanhellemont, M., Baeten, L., de la Peña, E., Bonte, D., Martel, A., Verheyen, K., Lens, L., 2017. Tree species identity outweighs the effects of tree species diversity and forest fragmentation on understorey diversity and composition. Plant Ecology and Evolution 150, 229–239. https://doi.org/10.5091/plecevo.2017.1331

De Pauw, K., Depauw, L., Calders, K., Caluwaerts, S., Cousins, S.A.O., De Lombaerde, E., Diekmann, M., Frey, D., Lenoir, J., Meeussen, C., Orczewska, A., Plue, J., Spicher, F., Zellweger, F., Vangansbeke, P., Verheyen, K., De Frenne, P., 2023. Urban forest microclimates across temperate Europe are shaped by deep edge effects and forest structure. Agricultural and Forest Meteorology 341, 109632. https://doi.org/10.1016/j.agrformet.2023.109632

Deilami, K., Kamruzzaman, Md., Liu, Y., 2018. Urban heat island effect: A systematic review of spatio-temporal factors, data, methods, and mitigation measures. International Journal of Applied Earth Observation and Geoinformation 67, 30–42. https://doi.org/10.1016/j.jag.2017.12.009

Ebi, K.L., Capon, A., Berry, P., Broderick, C., de Dear, R., Havenith, G., Honda, Y., Kovats, R.S., Ma, W., Malik, A., Morris, N.B., Nybo, L., Seneviratne, S.I., Vanos, J., Jay, O., 2021. Hot weather and heat extremes: health risks. The Lancet 398, 698–708. https://doi.org/10.1016/S0140-6736(21)01208-3

Frazer, G.W., Canham, C.D., Lertzman, K.P., 1999. Gap Light Analyzer (GLA), Version 2.0: Imaging software to extract canopy structure and gap light transmission indices from true-colour fisheye photographs, users manual and program documentation. Simon Fraser University, Burnaby, British Columbia, and the Institute of Ecosystem Studies, Millbrook, New York 36.

Geletič, J., Lehnert, M., Resler, J., Krč, P., Middel, A., Krayenhoff, E.S., Krüger, E., 2022. High-fidelity simulation of the effects of street trees, green roofs and green walls on the distribution of thermal exposure in Prague-Dejvice. Building and Environment 223, 109484. https://doi.org/10.1016/j.buildenv.2022.109484

Gillerot, L., Landuyt, D., Oh, R., Chow, W., Haluza, D., Ponette, Q., Jactel, H., Bruelheide, H., Jaroszewicz, B., Scherer-Lorenzen, M., De Frenne, P., Muys, B., Verheyen, K., 2022. Forest structure and composition alleviate human thermal stress. Global Change Biology 28, 7340–7352. https://doi.org/10.1111/gcb.16419
Harlan, S.L., Brazel, A.J., Prashad, L., Stefanov, W.L., Larsen, L., 2006. Neighborhood microclimates and vulnerability to heat stress. Social Science & Medicine 63, 2847–2863. https://doi.org/10.1016/j.socscimed.2006.07.030
He, X., Miao, S., Shen, S., Li, J., Zhang, B., Zhang, Z., Chen, X., 2015. Influence of sky view factor on outdoor thermal environment and physiological equivalent temperature. Int J Biometeorol 59, 285–297. https://doi.org/10.1007/s00484-014-0841-5
Höppe, P., 1999. The physiological equivalent temperature - a universal index for the biometeorological assessment of the thermal environment. International Journal of Biometeorology 43, 71–75. https://doi.org/10.1007/s004840050118
ISO, 1998. ISO 7726:1998 Ergonomics of the thermal environment-Instruments for measuring physical quantities. International Standard Organization for Standardization, Geneva, Switzerland.
Iungman, T., Cirach, M., Marando, F., Barboza, E.P., Khomenko, S., Masselot, P., Quijal-Zamorano, M., Mueller, N., Gasparrini, A., Urquiza, J., Heris, M., Thondoo, M., Nieuwenhuijsen, M., 2023. Cooling cities through urban green infrastructure: a health impact assessment of European cities. The Lancet 0. https://doi.org/10.1016/S0140-6736(22)02585-5
Johansson, E., Thorsson, S., Emmanuel, R., Krüger, E., 2014. Instruments and methods in outdoor thermal comfort studies – The need for standardization. Urban Climate, ICUC8: The 8th International Conference on Urban Climate and the 10th Symposium on the Urban Environment 10, 346–366. https://doi.org/10.1016/j.uclim.2013.12.002
Kleerekoper, L., van Esch, M., Salcedo, T.B., 2012. How to make a city climate-proof, addressing the urban heat island effect. Resources, Conservation and Recycling, Climate Proofing Cities 64, 30–38. https://doi.org/10.1016/j.resconrec.2011.06.004
KMI, 2022. Klimatologisch seizoenoverzicht zomer 2022. Koninklijk Meteorologisch Instituut van België, Ukkel, Brussel.
Konijnendijk, C., 2021. The 3-30-300 Rule for Urban Forestry and Greener Cities. Biophilic Cities Journal 4, 2.
Krayenhoff, E.S., Broadbent, A.M., Zhao, L., Georgescu, M., Middel, A., Voogt, J.A., Martilli, A., Sailor, D.J., Erell, E., 2021. Cooling hot cities: a systematic and critical review of the numerical modelling literature. Environ. Res. Lett. 16, 053007. https://doi.org/10.1088/1748-9326/abdcf1
Krüger, E., Ihlenfeld, W., Leder, S., Lima, L.C., 2023. Application of microcontroller-based systems in human biometeorology studies: a bibliometric analysis. Int J Biometeorol. https://doi.org/10.1007/s00484-023-02518-z
Landsberg, H.E., Maisel, T.N., 1972. Micrometeorological observations in an area of urban growth. Boundary-Layer Meteorol 2, 365–370. https://doi.org/10.1007/BF02184776
Lee, H., Mayer, H., Chen, L., 2016. Contribution of trees and grasslands to the mitigation of human heat stress in a residential district of Freiburg, Southwest Germany. Landscape and Urban Planning 148, 37–50. https://doi.org/10.1016/j.landurbplan.2015.12.004
Lehnert, M., Tokar, V., Jurek, M., Geletič, J., 2020. Summer thermal comfort in Czech cities: measured effects of blue and green features in city centres. Int J Biometeorol. https://doi.org/10.1007/s00484-020-02010-y
Lenton, T.M., Xu, C., Abrams, J.F., Ghadiali, A., Loriani, S., Sakschewski, B., Zimm, C., Ebi, K.L., Dunn, R.R., Svenning, J.-C., Scheffer, M., 2023. Quantifying the human cost of global warming. Nat Sustain 1–11. https://doi.org/10.1038/s41893-023-01132-6
Matzarakis, A., Mayer, H., Iziomon, M.G., 1999. Applications of a universal thermal index: physiological equivalent temperature. International Journal of Biometeorology 43, 76–84. https://doi.org/10.1007/s004840050119
Matzarakis, A., Rutz, F., Mayer, H., 2010. Modelling radiation fluxes in simple and complex environments: basics of the RayMan model. Int J Biometeorol 54, 131–139. https://doi.org/10.1007/s00484-009-0261-0

Matzarakis, A., Rutz, F., Mayer, H., 2007. Modelling radiation fluxes in simple and complex environments—application of the RayMan model. Int J Biometeorol 51, 323–334. https://doi.org/10.1007/s00484-006-0061-8

Mayer, H., Höppe, P., 1987. Thermal comfort of man in different urban environments. Theor Appl Climatol 38, 43–49. https://doi.org/10.1007/BF00866252

Mora, C., Dousset, B., Caldwell, I.R., Powell, F.E., Geronimo, R.C., Bielecki, C.R., Counsell, C.W.W., Dietrich, B.S., Johnston, E.T., Louis, L.V., Lucas, M.P., McKenzie, M.M., Shea, A.G., Tseng, H., Giambelluca, T.W., Leon, L.R., Hawkins, E., Trauernicht, C., 2017. Global risk of deadly heat. Nature Clim Change 7, 501–506. https://doi.org/10.1038/nclimate3322

Nichol, J., 2005. Remote Sensing of Urban Heat Islands by Day and Night. Photogrammetric Engineering & Remote Sensing 71, 613–621. https://doi.org/10.14358/PERS.71.5.613

Nikolopoulou, M., Baker, N., Steemers, K., 1999. Improvements to the Globe Thermometer for Outdoor Use. Architectural Science Review 42, 27–34. https://doi.org/10.1080/00038628.1999.9696845

Obradovich, N., Migliorini, R., Mednick, S.C., Fowler, J.H., 2017. Nighttime temperature and human sleep loss in a changing climate. Science Advances 3, e1601555. https://doi.org/10.1126/sciadv.1601555

Oke, T.R., 1973. City Size and the Urban Heat Island. Atmospheric Environment 7, 769–779.

Pinheiro, J., Bates, D., Debroy, S., Sarkar, D., R Core Team, 2021. nlme: Linear and Nonlinear Mixed Effects Models.

Potchter, O., Cohen, P., Lin, T.-P., Matzarakis, A., 2018. Outdoor human thermal perception in various climates: A comprehensive review of approaches, methods and quantification. Science of The Total Environment 631–632, 390–406. https://doi.org/10.1016/j.scitotenv.2018.02.276

R Core Team, 2023. R: A language and environment for statistical computing.

Rahman, M.A., Stratopoulos, L.M.F., Moser-Reischl, A., Zölch, T., Häberle, K.-H., Rötzer, T., Pretzsch, H., Pauleit, S., 2020. Traits of trees for cooling urban heat islands: A meta-analysis. Building and Environment 170, 106606. https://doi.org/10.1016/j.buildenv.2019.106606

Ren, Z., Zhao, H., Fu, Y., Xiao, L., Dong, Y., 2021. Effects of urban street trees on human thermal comfort and physiological indices: a case study in Changchun city, China. J. For. Res. https://doi.org/10.1007/s11676-021-01361-5

Resler, J., Eben, K., Geletič, J., Krč, P., Rosecký, M., Sühring, M., Belda, M., Fuka, V., Halenka, T., Huszár, P., Karlický, J., Benešová, N., Ďoubalová, J., Honzáková, K., Keder, J., Nápravníková, Š., Vlček, O., 2021. Validation of the PALM model system 6.0 in a real urban environment: a case study in Dejvice, Prague, the Czech Republic. Geoscientific Model Development 14, 4797–4842. https://doi.org/10.5194/gmd-14-4797-2021

Romanello, M., Di Napoli, C., Drummond, P., Green, C., Kennard, H., Lampard, P., Scamman, D., Arnell, N., Ayeb-Karlsson, S., Ford, L.B., Belesova, K., Bowen, K., Cai, W., Callaghan, M., Campbell-Lendrum, D., Chambers, J., van Daalen, K.R., Dalin, C., Dasandi, N., Dasgupta, S., Davies, M., Dominguez-Salas, P., Dubrow, R., Ebi, K.L., Eckelman, M., Ekins, P., Escobar, L.E., Georgeson, L., Graham, H., Gunther, S.H., Hamilton, I., Hang, Y., Hänninen, R., Hartinger, S., He, K., Hess, J.J., Hsu, S.-C., Jankin, S., Jamart, L., Jay, O., Kelman, I., Kiesewetter, G., Kinney, P., Kjellstrom, T., Kniveton, D., Lee, J.K.W., Lemke, B., Liu, Y., Liu, Z., Lott, M., Batista, M.L., Lowe, R., MacGuire, F., Sewe, M.O., Martinez-Urtaza, J., Maslin, M., McAllister, L., McGushin, A., McMichael, C., Mi, Z., Milner, J., Minor, K., Minx, J.C., Mohajeri, N., Moradi-Lakeh, M., Morrissey, K., Munzert, S., Murray, K.A., Neville, T., Nilsson, M., Obradovich, N., O'Hare, M.B., Oreszczyn, T., Otto, M., Owfi, F., Pearman, O., Rabbaniha, M., Robinson, E.J.Z., Rocklöv, J., Salas, R.N., Semenza, J.C., Sherman, J.D., Shi, L., Shumake-Guillemot, J., Silbert, G., Sofiev, M., Springmann, M., Stowell, J., Tabatabaei, M., Taylor, J., Triñanes, J., Wagner, F., Wilkinson, P., Winning, M., Yglesias-González, M., Zhang, S., Gong, P., Montgomery, H., Costello, A., 2022. The 2022 report of the Lancet Countdown on health and climate change: health at the mercy of fossil fuels. The Lancet 400, 1619–1654. https://doi.org/10.1016/S0140-6736(22)01540-9

Royal Meteorological Institute of Belgium, 2023. Klimaatstatistieken van de Belgische gemeenten - Gent [WWW Document]. URL https://www.meteo.be/resources/climatology/climateCity/pdf/climate_INS44021_9120_nl.pdf (accessed 6.27.23).

Schwaab, J., Meier, R., Mussetti, G., Seneviratne, S., Bürgi, C., Davin, E.L., 2021. The role of urban trees in reducing land surface temperatures in European cities. Nat Commun 12, 6763. https://doi.org/10.1038/s41467-021-26768-w

Sharmin, M., Tjoelker, M.G., Pfautsch, S., Esperón-Rodriguez, M., Rymer, P.D., Power, S.A., 2023. Tree Traits and Microclimatic Conditions Determine Cooling Benefits of Urban Trees. Atmosphere 14, 606. https://doi.org/10.3390/atmos14030606

Stewart, I.D., Oke, T.R., 2012. Local Climate Zones for Urban Temperature Studies. Bulletin of the American Meteorological Society 93, 1879–1900. https://doi.org/10.1175/BAMS-D-11-00019.1

Taleghani, M., 2018. Outdoor thermal comfort by different heat mitigation strategies- A review. Renewable and Sustainable Energy Reviews 81, 2011–2018. https://doi.org/10.1016/j.rser.2017.06.010

Tamaskani Esfehankalateh, A., Ngarambe, J., Yun, G.Y., 2021. Influence of Tree Canopy Coverage and Leaf Area Density on Urban Heat Island Mitigation. Sustainability 13, 7496. https://doi.org/10.3390/su13137496

Thorsson, S., Lindberg, F., Eliasson, I., Holmer, B., 2007. Different methods for estimating the mean radiant temperature in an outdoor urban setting. International Journal of Climatology 27, 1983–1993. https://doi.org/10.1002/joc.1537

Top, S., Milošević, D., Caluwaerts, S., Hamdi, R., Savić, S., 2020. Intra-urban differences of outdoor thermal comfort in Ghent on seasonal level and during record-breaking 2019 heat wave. Building and Environment 185, 107103. https://doi.org/10.1016/j.buildenv.2020.107103

Turner, V.K., Middel, A., Vanos, J.K., 2023. Shade is an essential solution for hotter cities. Nature 619, 694–697. https://doi.org/10.1038/d41586-023-02311-3

Tzavali, A., Paravantis, J.P., Mihalakakou, G., Fotiadi, A., Stigka, E., 2015. Urban heat island intensity: A literature review. Fresenius Environmental Bulletin 24, 4537–4554.

United Nations, 2019. World urbanization prospects: the 2018 revision.

van Hove, L.W.A., Jacobs, C.M.J., Heusinkveld, B.G., Elbers, J.A., van Driel, B.L., Holtslag, A.A.M., 2015. Temporal and spatial variability of urban heat island and thermal comfort within the Rotterdam agglomeration. Building and Environment, Special Issue: Climate adaptation in cities 83, 91–103. https://doi.org/10.1016/j.buildenv.2014.08.029

Vanos, J.K., Wright, M.K., Kaiser, A., Middel, A., Ambrose, H., Hondula, D.M., 2022. Evaporative misters for urban cooling and comfort: effectiveness and motivations for use. Int J Biometeorol 66, 357–369. https://doi.org/10.1007/s00484-020-02056-y

Wang, W., Zhang, B., Zhou, W., Lv, H., Xiao, L., Wang, H., Du, H., He, X., 2019. The effect of urbanization gradients and forest types on microclimatic regulation by trees, in association with climate, tree sizes and species compositions in Harbin city, northeastern China. Urban Ecosyst 22, 367–384. https://doi.org/10.1007/s11252-019-0823-9

Wanka, A., Arnberger, A., Allex, B., Eder, R., Hutter, H.-P., Wallner, P., 2014. The challenges posed by climate change to successful ageing. Z Gerontol Geriat 47, 468–474. https://doi.org/10.1007/s00391-014-0674-1

Wong, N.H., Tan, C.L., Kolokotsa, D.D., Takebayashi, H., 2021. Greenery as a mitigation and adaptation strategy to urban heat. Nat Rev Earth Environ 2, 166–181. https://doi.org/10.1038/s43017-020-00129-5

Yan, H., Wu, F., Nan, X., Han, Q., Shao, F., Bao, Z., 2022. Influence of view factors on intra-urban air temperature and thermal comfort variability in a temperate city. Science of The Total Environment 841, 156720. https://doi.org/10.1016/j.scitotenv.2022.156720

Zellweger, F., Coomes, D., Lenoir, J., Depauw, L., Maes, S.L., Wulf, M., Kirby, K.J., Brunet, J., Kopecký, M., Máliš, F., Schmidt, W., Heinrichs, S., Ouden, J. den, Jaroszewicz, B., Buyse, G., Spicher, F., Verheyen, K., Frenne, P.D., 2019. Seasonal drivers of understorey temperature buffering in temperate deciduous forests across Europe. Global Ecology and Biogeography 28, 1774–1786. https://doi.org/10.1111/geb.12991

Ziter, C.D., Pedersen, E.J., Kucharik, C.J., Turner, M.G., 2019. Scale-dependent interactions between tree canopy cover and impervious surfaces reduce daytime urban heat during summer. Proceedings of the National Academy of Sciences 116, 7575–7580. https://doi.org/10.1073/pnas.1817561116

Zuur, A.F., Ieno, E.N., Walker, N.J., Saveliev, A.A., Smith, G.M., 2009. Mixed effects models and extensions in ecology with R. Springer.

Fig. 1 | Map (A) with the locations of the 17 microclimate stations (B) measuring air temperature, air humidity, grey globe temperature and wind speed. Locations span a gradient from dense forest stands (C) to fully urbanised environments (D). © Google Maps.

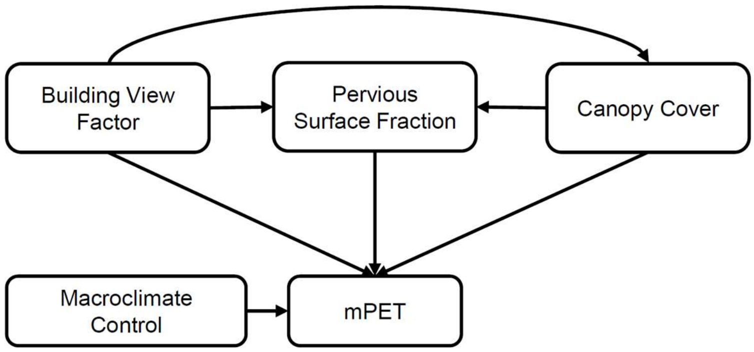

Fig. 2 | Directed Acyclic Graph (DAG) with the causal assumptions underlying our statistical model.

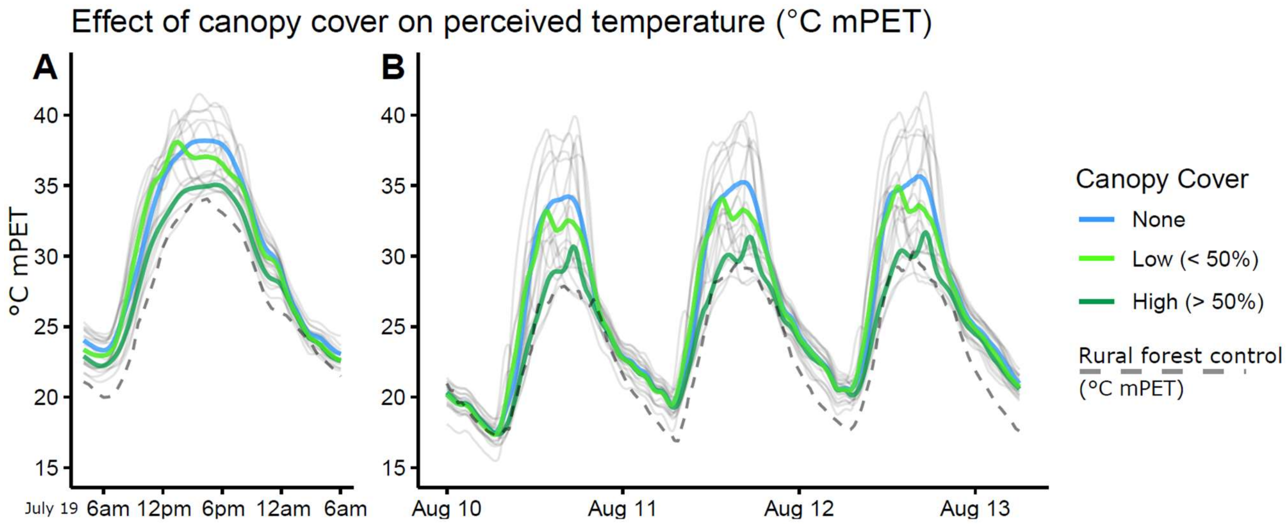

Fig. 3 | Trends in perceived temperature for the hottest day of 2022 (A) and three hot days during the second heatwave of 2022 (B). Each light grey line represents one of the 17 locations. Coloured lines represent average temperatures for locations grouped per canopy coverage. Control measures are averaged modified Physiologically Equivalent Temperature (mPET) data from ten nearby rural forests.

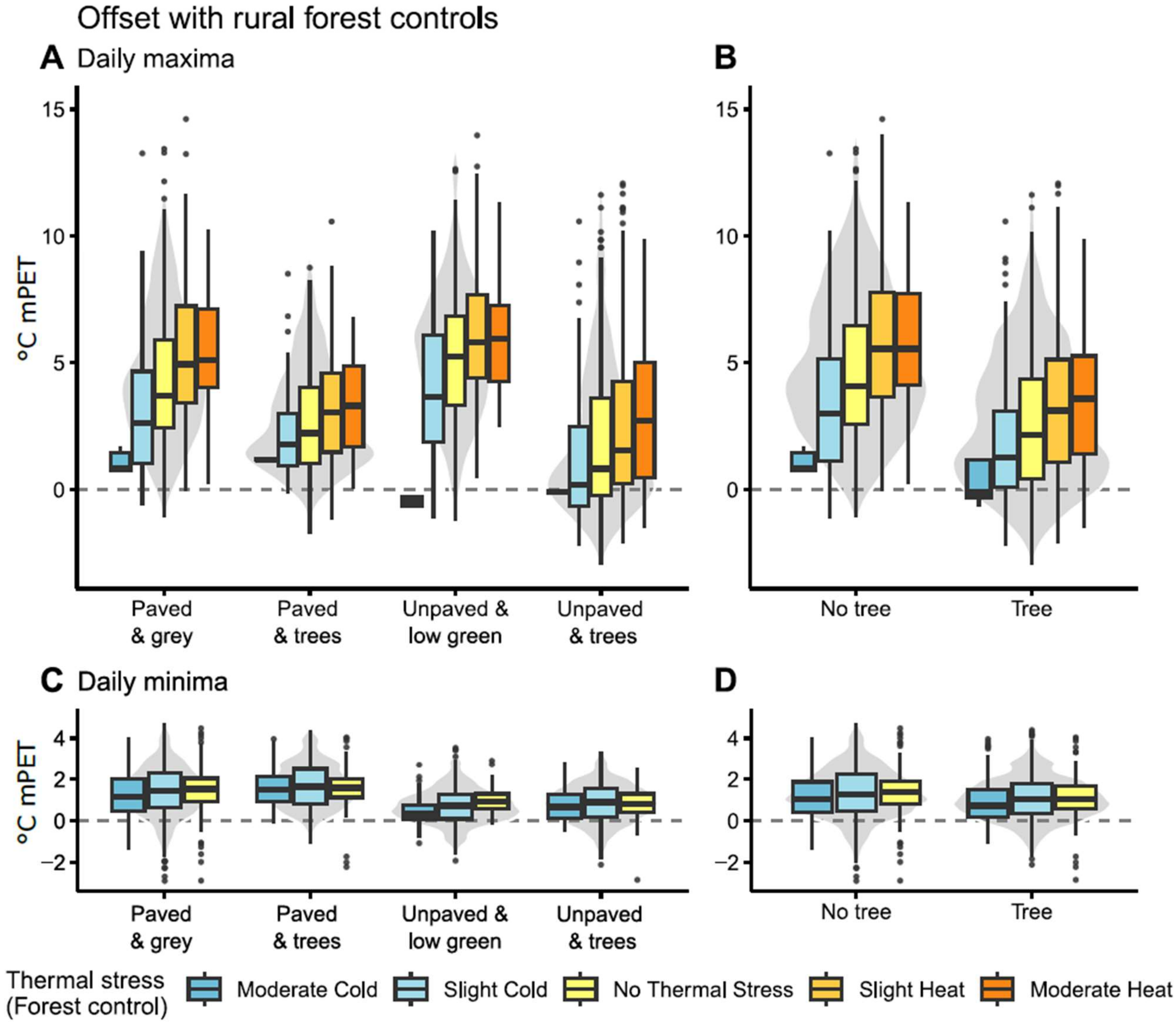

Fig. 4 | Offsets refer to the perceived temperature difference between urban locations minus rural forest controls, where positive values denote warmer urban conditions compared to rural forest controls. In left graphs (A-C), daily observations are grouped per location type and right (B-D) the same data are grouped according to the presence of trees in plots. mPET = modified Physiologically Equivalent Temperature.

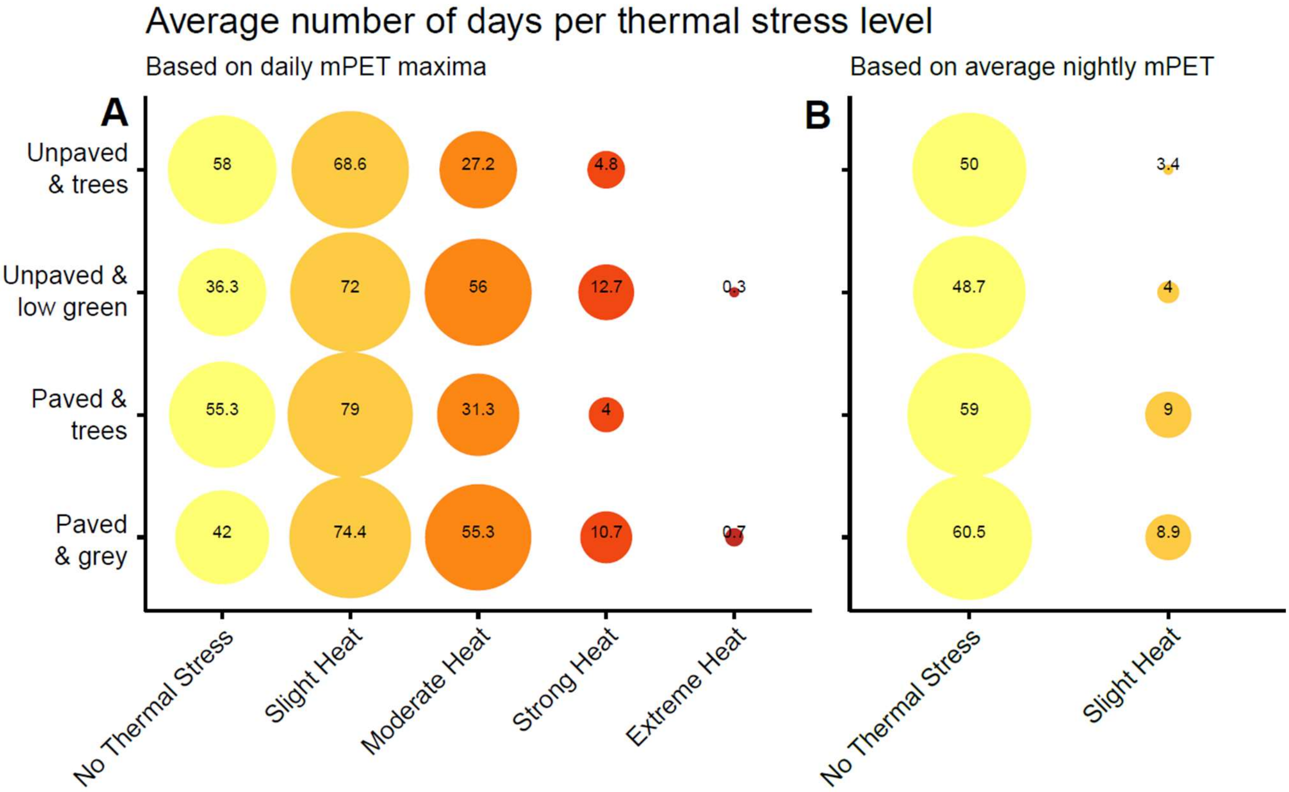

Fig. 5 | The average number of days with daily mPET maxima (A) or average nightly modified Physiologically Equivalent Temperature (mPET) (B) within heat stress categories, in function of location type. Circle sizes reflect the number of days, which represent an average of three to six locations per location type.

Table 1 | Overview of the 17 locations and average values of the rural forest controls. Percentages refer to the surface share within a circular plot with radius 10 m around the heat stress stations. LCZ = Local Climate Zone.

Location	Coordinates	Description	Canopy Cover	Building View Factor	Pervious Surface Fraction	Sky View Factor
Paved & grey						
IV1	51.051562, 3.702872	Predominantly paved parking surrounded by brick walls of *ca.* 2.5m height and some small flowering beds (LCZ 3).	0%	0%	15%	86%
IV2	51.052981, 3.707041	Next to a large university campus parking, half enclosed by buildings of *ca.* 10m height (LCZ 1).	0%	34%	0%	66%
IV3	51.0523569, 3.7062332	NS-exposed street next to primary school and residential buildings of *ca.* 10m height (LCZ 2).	0%	66%	0%	34%
IV4	51.054394, 3.707708	Narrow EW-exposed street with houses of *ca.* 7m height (LCZ 3).	0%	66%	0%	34%
IV5	51.0522932, 3.700859	Fully paved abandoned industrial site, next to a building of *ca.* 7m height. 'Greyest' location (LCZ 8).	0%	36%	0%	63%
IV6	51.051662, 3.70755	Very narrow EW-exposed street between houses of *ca.* 5m height with small flowerbed (LCZ 3).	0%	69%	1%	31%
Paved & trees						
LV1	51.052068, 3.707386	Unpaved roundabout surrounded by asphalted streets, with two mature trees (LCZ 3_B).	80%	4%	25%	23%
LV2	51.0518975, 3.7065614	NS-exposed street between houses of *ca.* 8m, with mid-sized tree (LCZ 3_B).	15%	41%	5%	38%
LV3	51.054243, 3.707049	Narrow EW- exposed street with houses of *ca.* 7m and one young tree (LCZ 3_B).	10%	38%	0%	50%
Unpaved & low green						

LG1	51.054382, 3.705726	Private vegetable garden with between buildings of *ca.* 2m and a small wall of *ca.* 2m (LCZ 4_D).	0%	6%	100%	94%
LG2	51.053699, 3.708987	Lawn with tall grasses and forbs, between an array of small trees and a university building of *ca.* 11m with many windows (LCZ 5_D).	5%	23%	90%	77%
LG3	51.050522, 3.704597	Small neighbourhood park with patches of tall grasses and one small tree (LCZ 9_D).	10%	0%	100%	94%
Unpaved & trees						
HG1	51.055029, 3.707637	Pocket forest of around 40a with a moderate density of mature trees, next to a pond (LCZ A).	70%	0%	70%	18%
HG2	51.054851, 3.707533	Pocket forest of around 40a with a high density of mature trees (LCZ A).	100%	0%	95%	12%
HG3	51.050689, 3.705224	Private garden with a moderate density of mature trees (LCZ 6_A).	75%	0%	100%	19%
HG4	51.0526691, 3.7067036	Campus vegetable garden surrounded by a lawn and three large trees (LCZ 9_B).	40%	0%	100%	56%
HG5	51.054537, 3.707286	Lawn with three young trees, next to a brick wall of *ca*. 2m (LCZ 5_B).	40%	2%	95%	68%
Rural forest controls		Ten mature managed forest stands composed of European beech (*Fagus sylvatica*), pedunculate oak (*Quercus robur*) and/or red oak (*Q. rubra*) with a canopy height of 30 - 35m.	100%	0%	100%	9%